

# Creating the optical bistable switch in the dielectric slab doped with asymmetric semiconductor quantum wells

R. NASEHI

Young Researchers and Elite Club, Central Tehran Branch, Islamic Azad University, Tehran, Iran;  
e-mail address: rajab.naseh@gmail.com

We have investigated the optical switching in a dielectric slab with a novel configuration of solid-state medium. This new scheme combines the attractive features of all-optical switching in dielectric medium doped with asymmetric quantum well nanostructure with the ability to convert the optical bistability to multistability (or *vice versa*) by using the strength of Fano interference and the energy splitting effect. The dependence of optical bistability behavior on the intensity of the strong coupling field and the slab thickness is also given.

Keywords: optical bistability, optical multistability, dielectric slab.

## 1. Introduction

It is well-known that many kinds of optical phenomena based on the quantum coherence and quantum interference are the basic mechanisms in semiconductor quantum wells (SQWs), investigated extensively in recent years. There has been much interest in a variety of new optical phenomena based on the quantum interference effect such as coherent population trapping [1], enhanced index of refraction [2, 3], electromagnetically induced transparency [4–6], enhancing Kerr nonlinearity [7], optical soliton [8, 9], optical bistability (OB) and optical multistability (OM) [10–14]. SADEGHI *et al.* [15] showed that electromagnetically induced transparency (EIT) may be obtained in an asymmetric QW with appropriate driving fields, provided that the coherence between the intersubbands considered is preserved for a sufficiently long time. Propagation of light in solid-state material, such as a slab system or photonic crystal (PC), is also important due to their potential applications. Propagation of an electromagnetic field in one-dimensional PCs (1DPCs) has attracted a lot of attention in recent years. In fact, periodic media called PCs are an important material for the optical properties of a light pulse [16, 17]. A multi-layered medium is considered as a simple example of the 1DPCs. In the past three decades, optical transistors and all-optical switches based on OB in two and three-level atomic systems have been extensively studied both experimentally and

theoretically [18–20]. OB processes were done in hot atoms rather than in cold atomic media theoretically and experimentally in recent years [21, 22]. It is worth pointing out that JOSHI and XIAO recently have analyzed the OB behavior in a SQW that interacts with two electromagnetic fields, a strong field and a weak field, and showed that the threshold for switching to upper branch of the bistable curve can be reduced due to the presence of quantum interference [23]. OB behavior based on intersubband transitions in an asymmetric coupled quantum well (CQW) driven by laser fields in the unidirectional ring cavity is analyzed in [24]. So quantum coherence and interference in QW structures have attracted great interest due to their potentially important applications in optoelectronics and solid-state quantum information science. In fact, phenomena such as modified Rabi oscillations and controlled population transfer [25], ultra-fast all-optical switching [26], and other novel phenomena [27] have been theoretically investigated and experimentally displayed. Devices which take advantage of intersubband transitions in QWs have inherent advantages which the atomic systems do not have such as large electric dipole moments due to small effective electron mass, and a great flexibility in the device design through a proper selection of the materials and their sizes.

Our investigation on the four level system are based on the [28, 29], while our results are different from those proposals. ZHIPING WANG [30] proposed that the transient gain-absorption of the probe field in asymmetric SQWs can be controlled by intensity coupling field and the strength of Fano interference. However, to our best knowledge no related theoretical or experimental work has been carried out to study OB or multistability in asymmetric QWs doped into the dielectric slab, which has motivated us to carry out this research. Here, it should be pointed out that Fano interference through a tunneling barrier is used for an efficient and convenient manipulation of the OB and OM via various parameters in a slab which is doped by a SQW. Therefore, previous investigations into OB generation in gaseous, QW and quantum dot medium are usually based on the coherence induced by a strong external driven field and so are substantially different from our proposed scheme based on a dielectric slab.

## 2. Model and equations

### 2.1. Pulse propagation in a slab

We consider a weakly absorbing and nonmagnetic slab which is extended from  $z = 0$  to  $z = d$  in the  $z$  direction with the complex relative permittivity  $\varepsilon(\omega_p) = \varepsilon_r + i\varepsilon_i$  where  $\varepsilon_r$  and  $\varepsilon_i$  represent the dispersion and the absorption parts, respectively, as depicted in Fig. 1. Both sides of the slab are vacuums and a light pulse with Gaussian form at the surface of the slab in plane  $z = 0$ , incident on it. The transfer matrix of a normally incident monochromatic wave with frequency  $\omega_p$  is given by [31]

$$\begin{bmatrix} \cos(kd) & i \frac{1}{n(\omega_p)} \sin(kd) \\ in(\omega_p) \sin(kd) & \cos(kd) \end{bmatrix} \quad (1)$$

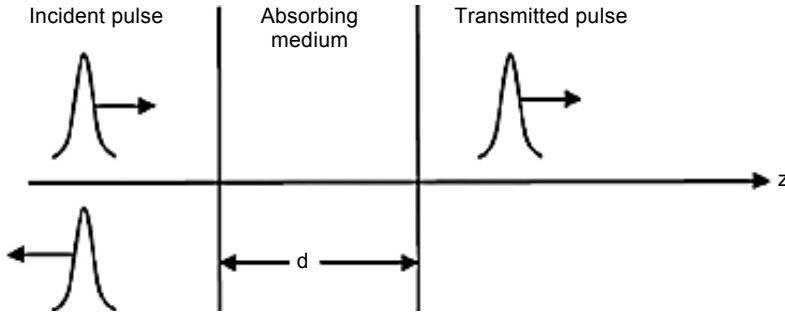


Fig. 1. Schematic of the weakly absorbing dielectric slab.

where  $n(\omega_p) = \sqrt{\varepsilon(\omega_p)}$  is the refractive index of the slab. We assume that the slab is doped by QD nanostructure, so the dielectric function, *i.e.*  $\omega_p$ , can be divided into two parts,

$$\varepsilon(\omega_p) = \varepsilon_b + \chi(\omega_p) \quad (2)$$

where  $\varepsilon_b = n_b^2$  is the background dielectric function and  $\chi(\omega_p)$  represents the susceptibility of the medium doped in the dielectric slab. Using the transfer-matrix method, the reflection and transmission coefficients of the monochromatic wave can be described as [32]

$$r(\omega_p) = \frac{-\frac{i}{2} \left( \frac{1}{\sqrt{\varepsilon}} - \sqrt{\varepsilon} \right) \sin(kd)}{\cos(kd) - \frac{i}{2} \left( \frac{1}{\sqrt{\varepsilon}} + \sqrt{\varepsilon} \right) \sin(kd)} \quad (3)$$

$$t(\omega_p) = \frac{1}{\cos(kd) - \frac{i}{2} \left( \frac{1}{\sqrt{\varepsilon}} + \sqrt{\varepsilon} \right) \sin(kd)} \quad (4)$$

These equations show that the susceptibility of the doped elements has a major role in determination of reflectivity and transmission of a light pulse through the slab. Moreover, these coefficients depend on the thickness and the refractive index of the slab. For the resonance condition, the thickness of the slab is employed as  $d = 2m\lambda_0 / (4\sqrt{\varepsilon_b})$ .

## 2.2. Quantum well system

We consider an asymmetric double SQW structure consisting of the subband in the shallow well  $|a\rangle$  and the subband in the deep well  $|b\rangle$ , which are separated by a narrow barrier as shown in Fig. 2a. The sample was grown as a 6.8 nm thick  $\text{Al}_{0.15}\text{Ga}_{0.85}\text{As}$  shallow well and a 7 nm thick GaAs deep well separated by a 2 nm thick  $\text{Al}_{0.3}\text{Ga}_{0.7}\text{As}$

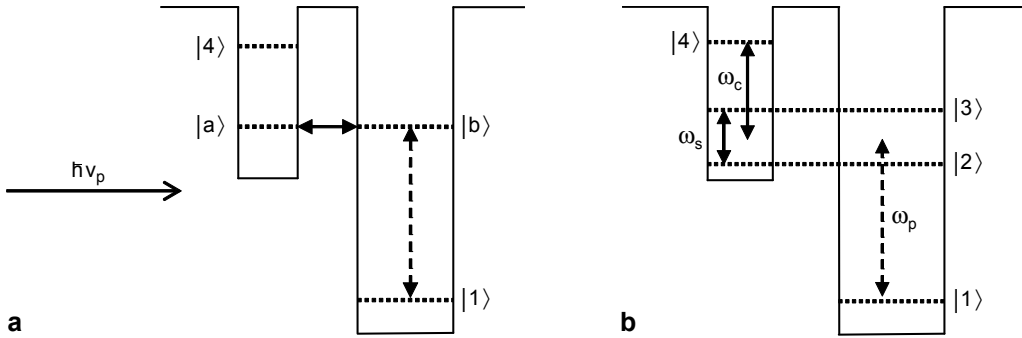


Fig. 2. Schematic band structure and level configuration of a double QW (a). Levels taken into account by Hamiltonian model and the basis of states used to describe it (b). The lower and higher subbands in the deep and shallow wells are denoted by levels  $|1\rangle$  and  $|4\rangle$ , respectively.

tunnel barrier, which due to the mixing of the states  $|a\rangle$  and  $|b\rangle$ , and under exactly resonant conditions leads to  $|2\rangle = (|a\rangle - |b\rangle)/\sqrt{2}$  and  $|3\rangle = (|a\rangle + |b\rangle)/\sqrt{2}$ . The splitting  $\omega_p$  on resonance is given by the coupling strength and can be controlled by adjusting the height and width of the tunneling barrier with applied bias voltage [33]. The lower subband in the deep well is denoted by level  $|1\rangle$ , and the higher subband in the shallow well is represented by level  $|4\rangle$  (see Fig. 2b). A weak probe laser field with frequency  $\omega_p$  (amplitude  $E_p$ ) and Rabi-frequencies  $\Omega_{p_1} = \wp_{21} E_p / 2\hbar$  and  $\Omega_{p_2} = \wp_{31} E_p / 2\hbar$  drive the transitions  $|1\rangle \leftrightarrow |2\rangle$  and  $|1\rangle \leftrightarrow |3\rangle$ , respectively, where  $\wp_{21}$  and  $\wp_{31}$  are the relevant intersubband dipole moments. Also,  $\Omega_{c_1} = \wp_{42} E_c / 2\hbar$  and  $\Omega_{c_2} = \wp_{43} E_c / 2\hbar$  are the corresponding Rabi-frequencies of the strong coupling field to transitions  $|4\rangle \leftrightarrow |i\rangle$  ( $i = 2, 3$ ), where  $E_c$  is the amplitude of strong coupling field and  $\wp_{4i}$  are the relevant intersubband dipole moments. The interaction Hamiltonian of the system is given by

$$H = H_0 + H_1 + H_2 \quad (5)$$

where  $H_0$  stands for free-energy part,  $H_1$  and  $H_2$  display the interaction of probe laser field and coherent coupling field with QW states, respectively. The detailed form of these terms can be written as

$$H_0 = \hbar\omega_1|1\rangle\langle 1| + \hbar\omega_2|2\rangle\langle 2| + \hbar\omega_3|3\rangle\langle 3| + \hbar\omega_4|4\rangle\langle 4| \quad (6)$$

$$H_1 = -\hbar\Omega_{p_1} \exp(-iv_p t)|1\rangle\langle 2| - \hbar\Omega_{p_2} \exp(-iv_p t)|1\rangle\langle 3| + \text{c.c.} \quad (7)$$

$$H_2 = -\hbar\Omega_{c_1} \exp(-iv_c t)|4\rangle\langle 2| - \hbar\Omega_{c_2} \exp(-iv_c t)|4\rangle\langle 3| + \text{c.c.} \quad (8)$$

Using the density operator, the time evolution of the system is governed by the Liouville equation which leads to the following equations of motion for the density matrix elements:

$$\begin{aligned} \dot{\rho}_{22} = & \gamma_{42}\rho_{44} - \gamma_2\rho_{22} - i\Omega_p(\rho_{21} - \rho_{12}) - i\Omega_c(\rho_{24} - \rho_{42}) + \\ & - \frac{1}{2}p\sqrt{\Gamma_{12}\Gamma_{13}}(\rho_{23} + \rho_{32}) \end{aligned} \quad (9a)$$

$$\begin{aligned} \dot{\rho}_{33} = & \gamma_{43}\rho_{44} - \gamma_3\rho_{33} - i\Omega_p(\rho_{31} - \rho_{13}) - i\Omega_c(\rho_{34} - \rho_{43}) + \\ & - \frac{1}{2}p\sqrt{\Gamma_{12}\Gamma_{13}}(\rho_{23} + \rho_{32}) \end{aligned} \quad (9b)$$

$$\dot{\rho}_{44} = -\gamma_4\rho_{44} - i\Omega_c(\rho_{42} - \rho_{24} + \rho_{43} - \rho_{34}) \quad (9c)$$

$$\begin{aligned} \dot{\rho}_{12} = & -\left[\left(\frac{\omega_s}{2} - \Delta_p\right)i + \frac{\Gamma_{12}}{2}\right]\rho_{12} - i\Omega_p(\rho_{11} - \rho_{22} - \rho_{32}) - i\Omega_c\rho_{14} + \\ & - \frac{1}{2}p\sqrt{\Gamma_{12}\Gamma_{13}}\rho_{13} \end{aligned} \quad (9d)$$

$$\begin{aligned} \dot{\rho}_{13} = & \left[\left(\frac{\omega_s}{2} + \Delta_p\right)i + \frac{\Gamma_{13}}{2}\right]\rho_{13} - i\Omega_p(\rho_{11} - \rho_{33} - \rho_{23}) - i\Omega_c\rho_{14} + \\ & - \frac{1}{2}p\sqrt{\Gamma_{12}\Gamma_{13}}\rho_{12} \end{aligned} \quad (9e)$$

$$\dot{\rho}_{14} = \left[\left(\Delta_c + \Delta_p\right)i - \frac{\Gamma_{14}}{2}\right]\rho_{14} + i\Omega_p(\rho_{34} + \rho_{24}) - i\Omega_c(\rho_{12} + \rho_{13}) \quad (9f)$$

$$\begin{aligned} \dot{\rho}_{23} = & \left(i\omega_s - \frac{\Gamma_{23}}{2}\right)\rho_{23} - i\Omega_p(\rho_{21} - \rho_{13}) - i\Omega_c(\rho_{24} - \rho_{43}) + \\ & - \frac{1}{2}p\sqrt{\Gamma_{12}\Gamma_{13}}(\rho_{22} + \rho_{33}) \end{aligned} \quad (9g)$$

$$\begin{aligned} \dot{\rho}_{24} = & \left[\left(\frac{\omega_s}{2} + \Delta_c\right)i - \frac{\Gamma_{24}}{2}\right]\rho_{24} + i\Omega_p\rho_{14} - i\Omega_c(\rho_{22} - \rho_{44} + \rho_{23}) + \\ & - \frac{1}{2}p\sqrt{\Gamma_{12}\Gamma_{13}}\rho_{34} \end{aligned} \quad (9h)$$

$$\begin{aligned} \dot{\rho}_{34} = & -\left[\left(\frac{\omega_s}{2} - \Delta_c\right)i - \frac{\Gamma_{34}}{2}\right]\rho_{34} + i\Omega_p\rho_{14} - i\Omega_c(\rho_{33} - \rho_{44} + \rho_{32}) + \\ & - \frac{1}{2}p\sqrt{\Gamma_{12}\Gamma_{13}}\rho_{24} \end{aligned} \quad (9i)$$

Here,  $\Delta_p = \delta_1 - \omega_p$  and  $\Delta_c = \delta_2 - \omega_c$  are the detuning between the frequencies of the probe and coupling laser fields and the average transition frequencies  $\delta_1 = (\omega_{12} + \omega_{13})/2$  and  $\delta_2 = (\omega_{42} + \omega_{43})/2$ . The energy splitting between the states  $|2\rangle$  and  $|3\rangle$  is denoted by  $\omega_s = E_3 - E_2$ , and given by the coherent coupling intensity of the tunneling. The population decay rates for the subband  $|i\rangle$ , denoted by  $\gamma_i$ , are due primarily to longitudinal optical (LO) phonon emission events at low temperature, and the total decay rates are given by  $\Gamma_{ij}$  ( $i \neq j$ ) [34, 35]. Because the subband  $|b\rangle$  is strongly coupled to a continuum via a thin barrier, the decay from state  $|b\rangle$  to the continuum inevitably results in these two dependent decay pathways: from the excited doublet to the common continuum. That is to say, the two decay pathways are related: the decay from one of the excited doublets can strongly affect the neighbouring transition, resulting in the interference characterized by those coupling terms. Such interference is similar to the decay induced coherence in atomic systems with two closely lying energy states and occurs due to quantum interference in the electronic continuum [33]. The intensity of the Fano interference [33] is defined by  $p = \eta / \sqrt{\Gamma_{12}\Gamma_{13}}$ , where the values  $p = 0$  and  $p = 1$  correspond to no interference and perfect interference, respectively, and  $\eta = \sqrt{\gamma_2\gamma_3}$  represents a coupling term between the states  $|3\rangle$  and  $|2\rangle$  via the LO phonon decay.

The nonlinear transfer matrix method produces the relation between transmitted pulse  $T$  and scaled dimensionless incident field intensity  $E_i$ . We used the expression  $I_i = (c\epsilon_0 E_i) / [2\text{Re}(\chi^{(3)})]$  for the incident field intensity. So, we summarize our results for the steady-state behavior of the output field intensity *versus* the input field intensity for various parameters illustrated in Figs. 3–6. Moreover, we show the behavior of output-input fields for various Fano interference. For the transmitted intensity  $U_t$  given parametrically, the incident intensity  $U_{in}$  is given by

$$U_{in} = U_t / T \quad (10)$$

### 3. Result and discussion

In the first step, we study the effect of coupling laser field  $\Omega_c$  which couples the upper level  $|4\rangle$  to the lower levels  $|3\rangle$  and  $|2\rangle$ . In Figure 3, we display the bistable behavior of probe field for different values of laser coupling field. Applied fields parameters are  $\Delta_p = 0.1\gamma$ ,  $\Delta_c = 0$ ,  $\Omega_c = 0.5\gamma$  (solid line),  $\Omega_c = 1\gamma$  (dotted line). An investigation in Fig. 3 shows that by increasing the intensity of laser coupling field  $\Omega_c$ , the OM is converted to OB. However, with the increasing laser coupling from  $0.5\gamma$  to  $1\gamma$ , the OM vanishes and changes to OB. This may be useful to control the hysteresis cycle width of the bistable curve simply by adjusting the intensity of the coupling field. In fact, for a low intensity of  $\Omega_c$ , the behavior of a four-level medium is similar to a usual three-level  $V$ -type medium. It can be found that by increasing the Fano interference, the threshold intensity of bistability is decreased (see Fig. 4). Finally, for the parameter  $p = 0.7$  (dotted line in Fig. 4) the bistability has disappeared and converts to the OM.

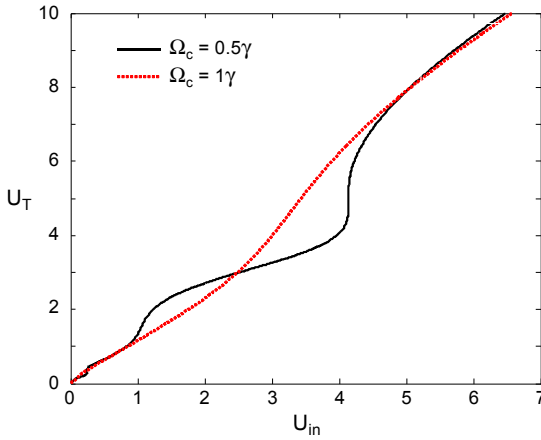


Fig. 3. Output field *versus* input field for different values of the coherent control field  $\Omega_c$ . Selected parameters are:  $\gamma_2 = 2.5\gamma$ ,  $\gamma_3 = 3\gamma$ ,  $\gamma_4 = 0.8\gamma$ ,  $\gamma_{42} = \gamma_{43} = 0.4\gamma$ ,  $\Gamma_{12} = 3\gamma$ ,  $\Gamma_{13} = 4\gamma$ ,  $\Gamma_{14} = 1.3\gamma$ ,  $\Gamma_{23} = 5\gamma$ ,  $\Gamma_{24} = 1\gamma$ ,  $\Gamma_{34} = 3.5\gamma$ ,  $\Delta_c = 0$ ,  $\Delta_p = 0.1\gamma$ ,  $\omega_s = 1\gamma$ ,  $\epsilon_b = 4$ ,  $m = 50$ ,  $p = 0.2$ ,  $\Omega_c = 0.5\gamma$  (solid line),  $\Omega_c = 1\gamma$  (dotted line).

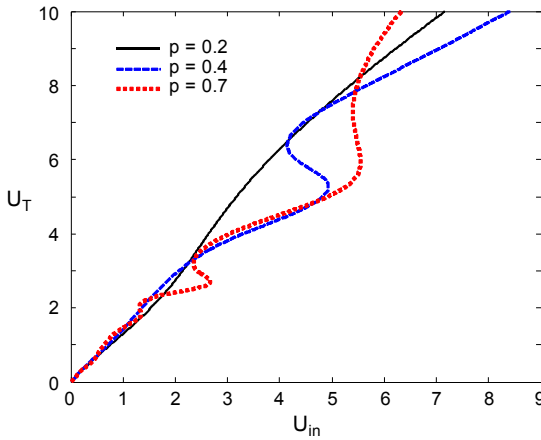


Fig. 4. Output field *versus* input field for different values of the Fano interference  $p$ . Selected parameters are:  $\Omega_c = 2\gamma$ ,  $\omega_s = 1\gamma$ ,  $p = 0.2$  (solid line),  $p = 0.4$  (dashed line),  $p = 0.7$  (dotted line). The other parameters the same as those of Fig. 3.

It can be realized that by adjusting the strength of the Fano interference, the switching from bistability to multistability or *vice versa* can be controlled. These different behaviors in OB and OM can be explained via the fact that the two decay pathways are related. The decay from one of the excited doublets can strongly affect the neighbouring transition, as a result of the interference characterized by those cross-coupling terms. Such interference is similar to the decay induced coherence in atomic systems

with two closely lying energy states and occurs due to quantum interference in the electronic continuum. It is worth noting that the behavior of OB in a slab doped with QW molecules is controlled (by applying the Fano interference), in respect to the free Fano interference. Physically, quantum interference will occur when at least there are two different ways to one final state which cannot be distinguished in principle. In the system considered here, there are interfering pathways of spontaneous emission from doublet levels, which affects the linear, nonlinear absorption and Kerr nonlinearity. Therefore, there are interfering pathways of spontaneous emission between two upper levels  $|2\rangle$ ,  $|3\rangle$  and lower level  $|1\rangle$ , leading to a reduction in the population in a lower level  $|1\rangle$ . Thus Kerr nonlinearity and nonlinear absorption are affected by quantum interference.

Figure 5 shows the dependence of the OB on the energy splitting of the levels  $|2\rangle$  and  $|3\rangle$ , in the presence of maximum Fano interference  $p = 0.7$ . It can be easily seen from curves of Fig. 5 that an increase in the value of  $\omega_s$  from  $1\gamma$  (solid line) to  $10\gamma$  (dotted line) leads to a gradual increase in the multistable threshold and finally OM is converted to OB. The reason for the above results can be qualitatively explained as follows. With increasing  $\omega_s$  between the energy levels  $|2\rangle$  and  $|3\rangle$ , the coupling efficiency of coherency decreases considerably. By applying an increasingly intense resonant tunneling through a thin barrier, the optical properties due to the intersubband transitions of the electronic medium can be controlled. As mentioned, the splitting on resonance is given by the coupling strength and can be controlled by adjusting the height and width of the tunneling barrier. Therefore, the behavior of OB can be tuned by appropriately adjusting the tunneling barrier. Consequently, when increasing  $\omega_s$ , the absorption for the probe laser at  $\Delta_p = 0.1\gamma$  can be destructed apparently as already verified from Figs. 5, which makes the cavity field hardly to reach saturation. This might be useful to manipulate the threshold value, converting OM to OB, and the hys-

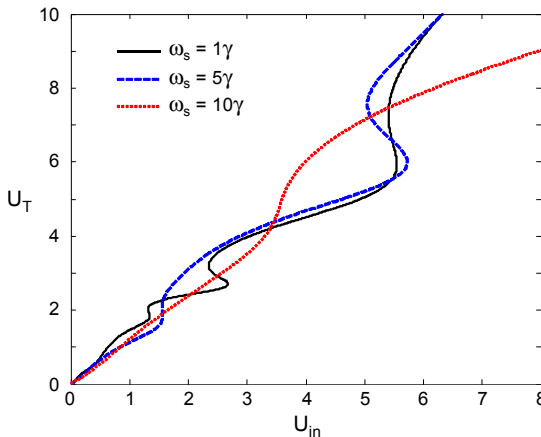


Fig. 5. Output field *versus* input field for different values of the energy splitting  $\omega_s$ . Selected parameters are:  $\Omega_c = 2\gamma$ ,  $p = 0.7$ ,  $\omega_s = 1\gamma$  (solid line),  $\omega_s = 5\gamma$  (dashed line),  $\omega_s = 10\gamma$  (dotted line). The other parameters the same as those of Fig. 3.

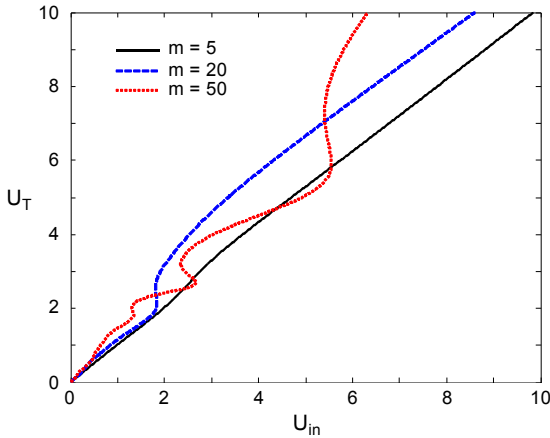


Fig. 6. Output field *versus* input field for different values of the thickness  $m$ . Selected parameters are:  $\Omega_c = 2\gamma$ ,  $p = 0.7$ ,  $m = 5$  (solid line),  $m = 20$  (dashed line),  $m = 50$  (dotted line). The other parameters the same as those of Fig. 3.

teresis cycle width of the bistable curve via varying  $\omega_s$ . In the next step, we study the effect of the thickness of the slab on the OB behavior of the probe field. The bistable behavior for different thickness is displayed in Fig. 6. It has been found out that the thickness of the slab has a major role in characterizing the bistable behavior, so that by increasing a thickness value, the OB is converted to OM only in the presence of maximum Fano interference. It is observed that for  $m = 5$ , the OB has vanished and for  $m = 20$ , the OB has appeared, while for a larger thickness value, *i.e.*,  $m = 50$ , the OB is converted to OM.

## 4. Conclusion

In summary, we have analyzed the bistable behavior in the dielectric slab doped with an asymmetric quantum well driven by a coherent coupling field and weak probe field inside a unidirectional ring cavity. It is clearly shown that the coupling field intensity and the strength of Fano interference can affect the OB and OM, which can be used to control the hysteresis loop of a bistable curve. In addition, the effects of the energy splitting and slab thickness on the behavior of a bistable curve are also discussed, and it is shown that the transition from OB to OM or *vice versa* can be realized by adjusting these parameters.

## References

- [1] ARIMONDO E., ORRIOLS G., *Nonabsorbing atomic coherences by coherent two-photon transitions in a three-level optical pumping*, Lettere al Nuovo Cimento **17**(10), 1976, pp. 333–338.
- [2] SCULLY M.O., *Enhancement of the index of refraction via quantum coherence*, Physical Review Letters **67**(14), 1991, p. 1855.
- [3] AIXI CHEN, *Influence of quantum coherence on propagation of a pulsed light in a triple quantum well*, Optics Express **19**(13), 2011, pp. 11944–11950.

- [4] SCULLY M.O., FLEISCHHAUER M., *Lasers without inversion*, Science **263**(5145), 1994, pp. 337–338.
- [5] KASH M.M., SAUTENKOV V.A., ZIBROV A.S., HOLLBERG L., WELCH G.R., LUKIN M.D., ROSTOVTSSEV Y., FRY E.S., SCULLY M.O., *Ultraslow group velocity and enhanced nonlinear optical effects in a coherently driven hot atomic gas*, Physical Review Letters **82**(26), 1999, p. 5229.
- [6] HARRIS S.E., *Electromagnetically induced transparency*, Physics Today **50**(7), 1997, p. 36.
- [7] YUEPING NIU, SHANGQING GONG, *Enhancing Kerr nonlinearity via spontaneously generated coherence*, Physical Review A **73**(5), 2006, article 053811.
- [8] YING WU, *Two-color ultraslow optical solitons via four-wave mixing in cold-atom media*, Physical Review A **71**(5), 2005, article 053820.
- [9] GUOXIANG HUANG, L. DENG, PAYNE M.G., *Dynamics of ultraslow optical solitons in a cold three-state atomic system*, Physical Review E **72**(1), 2005, article 016617.
- [10] HARSHAWARDHAN W., AGARWAL G.S., *Controlling optical bistability using electromagnetic-field-induced transparency and quantum interferences*, Physical Review A **53**(3), 1996, p. 1812.
- [11] ZHIPING WANG, MIAOCUN XU, *Control of the switch between optical multistability and bistability in three-level V-type atoms*, Optics Communications **282**(8), 2009, pp. 1574–1578.
- [12] YUAN CHEN, LI DENG, AIXI CHEN, *Controllable optical bistability and multistability in asymmetric double quantum wells via spontaneously generated coherence*, Annals of Physics **353**, 2015, pp. 1–8.
- [13] JOSHI A., MIN XIAO, *Optical multistability in three-level atoms inside an optical ring cavity*, Physical Review Letters **91**(14), 2003, article 143904.
- [14] JOSHI A., BROWN A., HAI WANG, MIN XIAO, *Controlling optical bistability in a three-level atomic system*, Physical Review A **67**(4), 2003, article 041801(R).
- [15] SADEGHI S.M., LEFFLER S.R., MEYER J., *Quantum interference and nonlinear optical processes in the conduction bands of infrared-coupled quantum wells*, Physical Review B **59**(23), 1999, p. 15388.
- [16] SOUK- OULIS C.M. [Ed.], *Photonic Band Gap and Localization*, Plenum, New York, 1993.
- [17] YABLONOVITCH E., GMITTER T.J., LEUNG K.M., *Photonic band structure: the face-centered-cubic case employing nonspherical atoms*, Physical Review Letters **67**(17), 1991, p. 2295.
- [18] GIBBS H.M., MCCALL S.L., VENKATESAN T.N.C., *Differential gain and bistability using a sodium-filled Fabry–Perot interferometer*, Physical Review Letters **36**(19), 1976, p. 1135.
- [19] OROZCO L.A., KIMBLE H.J., ROSENBERGER A.T., LUGIATO L.A., ASQUINI M.L., BRAMBILLA M., NARDUCCI L.M., *Single-mode instability in optical bistability*, Physical Review A **39**(3), 1989, p. 1235.
- [20] SAHRAI M., ASADPOUR S.H., SADIGHI-BONABI R., *Optical bistability via quantum interference from incoherent pumping and spontaneous emission*, Journal of Luminescence **131**(11), 2011, pp. 2395–2399.
- [21] JOSHI A., WENGE YANG, MIN XIAO, *Effect of quantum interference on optical bistability in the three-level V-type atomic system*, Physical Review A **68**(1), 2003, article 015806.
- [22] JIA-HUA LI, XIN-YOU LÜ, JING-MIN LUO, QIU-JUN HUANG, *Optical bistability and multistability via atomic coherence in an N-type atomic medium*, Physical Review A **74**(3), 2006, article 035801.
- [23] JOSHI A., XIAO M., *Optical bistability in a three-level semiconductor quantum-well system*, Applied Physics B: Lasers and Optics **79**(1), 2004, pp. 65–69.
- [24] JIA-HUA LI, *Coherent control of optical bistability in tunnel-coupled double quantum wells*, Optics Communications **274**(2), 2007, pp. 366–371.
- [25] BASTISTA A.A., CITRIN D.S., *Rabi flopping in a two-level system with a time-dependent energy renormalization: intersubband transitions in quantum wells*, Physical Review Letters **92**(12), 2004, article 127404.
- [26] SCHMIDT H., RAM R.J., *All-optical wavelength converter and switch based on electromagnetically induced transparency*, Applied Physics Letters **76**(22), 2000, p. 3173.
- [27] DYNES J.F., PASPALAKIS E., *Phase control of electron population, absorption, and dispersion properties of a semiconductor quantum well*, Physical Review B **73**(23), 2006, article 233305.
- [28] JIA-HUA LI, *Controllable optical bistability in a four-subband semiconductor quantum well system*, Physical Review B **75**(15), 2007, article 155329.
- [29] HUI SUN, YUEPING NIU, RUXIN LI, SHIQI JIN, SHANGQING GONG, *Tunneling-induced large cross-phase modulation in an asymmetric quantum well*, Optics Letters **32**(17), 2007, pp. 2475–2477.

- [30] ZHIPING WANG, *Transient gain-absorption of the probe field in asymmetric semiconductor quantum wells*, Optics Communications **283**(12), 2010, pp. 2552–2556
- [31] LI-GANG WANG, SHI-YAO ZHU, *Superluminal pulse reflection from a weakly absorbing dielectric slab*, Optics Letters **31**(14), 2006, pp. 2223–2225.
- [32] LI-GANG WANG, HONG CHEN, SHI-YAO ZHU, *Superluminal pulse reflection and transmission in a slab system doped with dispersive materials*, Physical Review E **70**(6), 2004, article 066602.
- [33] IMAMOĞLU A., RAM R.J., *Semiconductor lasers without population inversion*, Optics Letters **19**(21), 1994, pp. 1744–1746.
- [34] SERAPIGLIA G.B., PASPALAKIS E., SIRTORI C., VODOPYANOV K.L., PHILLIPS C.C., *Laser-induced quantum coherence in a semiconductor quantum well*, Physical Review Letters **84**(5), 2000, p. 1019.
- [35] TSUJINO S., BORAK A., MÜLLER E., SCHEINERT M., FALUB C.V., SIGG H., GRÜTZMACHER D., GIOVANNINI M., FAIST J., *Interface-roughness-induced broadening of intersubband electroluminescence in p-SiGe and n-GaInAs/AlInAs quantum-cascade structures*, Applied Physics Letters **86**(6), 2005, article 062113.

*Received January 9, 2016  
in revised form May 4, 2016*